

Stable operation of silicon photonic switches in field-deployed optical path network

Takayuki Kurosu^{a)}, Satoshi Suda, Hiroyuki Matsuura,
and Shu Namiki

National Institute of Advanced Industrial Science and Technology,
1-1-1 Umezono, Tsukuba, Ibaraki 305-8568, Japan

a) t.kurosu@aist.go.jp

Abstract: Optical switches based on silicon (Si) nanowire waveguide exhibit stable performance without active control of operating point owing to its extremely small size. To verify reliability, we carried out simultaneous operation of two Si-nanowire 8×8 optical switches in the optical path network that was deployed in Tokyo metropolitan area using dark fibres. System performance was studied transmitting 10-Gb/s WDM signals over two optical paths that were configured in a way that transmitted signals went through the 8×8 switches 10 times. Error free performance was achieved over a week without any adjustment of the switches.

Keywords: optical switch, silicon photonics, optical network, nanowire

Classification: Integrated optoelectronics

References

- [1] S. Namiki, *et al.*: “Ultrahigh-definition video transmission and extremely green optical networks for future,” *IEEE J. Sel. Top. Quantum Electron.* **17** (2011) 446 (DOI: [10.1109/JSTQE.2010.2051420](https://doi.org/10.1109/JSTQE.2010.2051420)).
- [2] S. Han, *et al.*: “Large-scale polarization-insensitive silicon photonic MEMS switches,” *J. Lightwave Technol.* **36** (2018) 1824 (DOI: [10.1109/JLT.2018.2791502](https://doi.org/10.1109/JLT.2018.2791502)).
- [3] S. Nakamura, *et al.*: “Optical switches based on silicon photonics for ROADM application,” *IEEE J. Sel. Top. Quantum Electron.* **22** (2016) 3600609 (DOI: [10.1109/JSTQE.2016.2569402](https://doi.org/10.1109/JSTQE.2016.2569402)).
- [4] K. Tanizawa, *et al.*: “Off-chip polarization-diversity 4×4 Si-wire optical switch with digital DGD compensation,” *IEEE Photonics Technol. Lett.* **28** (2016) 457 (DOI: [10.1109/LPT.2015.2499299](https://doi.org/10.1109/LPT.2015.2499299)).
- [5] K. Suzuki, *et al.*: “Broadband silicon photonics 8×8 switch based on double-Mach-Zehnder element switches,” *Opt. Express* **25** (2017) 7538 (DOI: [10.1364/OE.25.007538](https://doi.org/10.1364/OE.25.007538)).
- [6] T. Kurosu, *et al.*: “High-capacity multi-stage operation of polarization-diversity silicon photonics 8×8 optical switch,” *J. Lightw. Technol.* (2018) Early Access (DOI: [10.1109/JLT.2018.2865790](https://doi.org/10.1109/JLT.2018.2865790)).
- [7] L. Qiao, *et al.*: “ 32×32 silicon electro-optic switch with built-in monitors and balanced-status units,” *Sci. Rep.* **7** (2017) 42306 (DOI: [10.1038/srep42306](https://doi.org/10.1038/srep42306)).
- [8] P. Dumais, *et al.*: “Silicon photonic switch subsystem with 900 monolithically

- integrated calibration photodiodes and 64-fiber package,” J. Lightwave Technol. **36** (2018) 233 (DOI: [10.1109/JLT.2017.2755578](https://doi.org/10.1109/JLT.2017.2755578)).
- [9] H. Matsuura, *et al.*: “Accelerating switching speed of thermo-optic MZI silicon-photon switches with “turbo pulse” in PWM control,” Proc. OFC2017 (2017) W4E.3 (DOI: [10.1364/OFC.2017.W4E.3](https://doi.org/10.1364/OFC.2017.W4E.3)).
- [10] F. Futami, *et al.*: “Dynamic routing of Y-00 quantum stream cipher in deployed dynamic optical path network,” Proc. OFC2018 (2018) Tu2G.5 (DOI: [10.1364/OFC.2018.Tu2G.5](https://doi.org/10.1364/OFC.2018.Tu2G.5)).
- [11] K. Ishii, *et al.*: “Demonstration of fast cooperative operations in disaggregated optical node systems,” Proc. OFC2017 (2017) W1D.5 (DOI: [10.1364/OFC.2017.W1D.5](https://doi.org/10.1364/OFC.2017.W1D.5)).
- [12] K. Suzuki, *et al.*: “Polarization-rotator-free polarization-diversity 4×4 Si-wire optical switch,” IEEE Photon. J. **8** (2016) 0600707 (DOI: [10.1109/JPHOT.2016.2523985](https://doi.org/10.1109/JPHOT.2016.2523985)).

1 Introduction

Low-energy, high-throughput, optical switches are essential to realize ultra-low energy and ultra-low latency network based on dynamic optical path switching, which we call dynamic optical path network (DOPN) [1]. Among various type of optical switches, switches based on silicon photonics have advantages of high speed, high-density integration, mass production, and low cost [2, 3, 4]. Recently, we developed a polarization-insensitive 8×8 optical switch, which was based on silicon (Si) nanowire waveguide, double-Mach-Zehnder switch elements [5]. In this switch, off-chip polarization diversity is configured using two identical switch chips, which are only $1.7 \text{ mm} \times 7.7 \text{ mm}$. The 8×8 optical switch is assembled into 1RU blade to allow operation in the optical network with a power consumption of 18 W. Through multi-stage cascaded operation, it was confirmed that the switch had throughput of 48.2 Tb/s and an energy efficiency of 0.37 pJ/bit was achieved [6].

On the other hand, for long-term stable operation of the switch, a scheme is necessary to keep the switch elements in the optimum operating point under changing environment. Such a scheme usually involves temperature control of the switch chips and/or feedback control of each switch elements employing large number of monitoring photodiodes [7, 8]. The optical switch based on Si-nanowire waveguide technology, however, exhibits stable performance without any active control owing to extremely small size, which is advantageous for nulling the effect of environmental change. Actually, the switch elements constituting the 8×8 optical switch operate in the optimum condition by simply applying a constant bias offset, whose value is predetermined and stored in a look-up table [9].

For practical application of the switches, however, it is indispensable to confirm robustness and reliability through field operation. For this purpose, we constructed a DOPN testbed in Tokyo metropolitan area using deployed commercial fibre cables (dark fibres) and the Si-nanowire switch installed in central office. So far, the testbed has been utilized to demonstrate dynamic routing of quantum stream cipher taking advantage of signal format transparency, which is one of the attractive features of DOPN [10].

In this paper, we demonstrate, for the first time, simultaneous operation of two Si-nanowire 8×8 switches deployed in the commercial field of Tokyo metropolitan area. We studied transmission characteristics for two optical paths that were configured in such a way that transmitted signals went through Si-nanowire switches 10 times in total. Stable performance was observed without any adjustment of the switches for over a week, during which switching of two optical paths was performed.

2 Tokyo DOPN testbed

Fig. 1a shows the configuration of DOPN testbed, which was deployed in Tokyo metropolitan area. Currently, two sites (site-A and site-B) of author's institution (AIST in Tokyo Waterfront), the University of Tokyo and two private companies (company-A, -B) are linked to an optical node (Node-1), which is located in Ginza, by a pair of fibres. The optical node establishes an optical path between two end users as soon as it receives user's request.

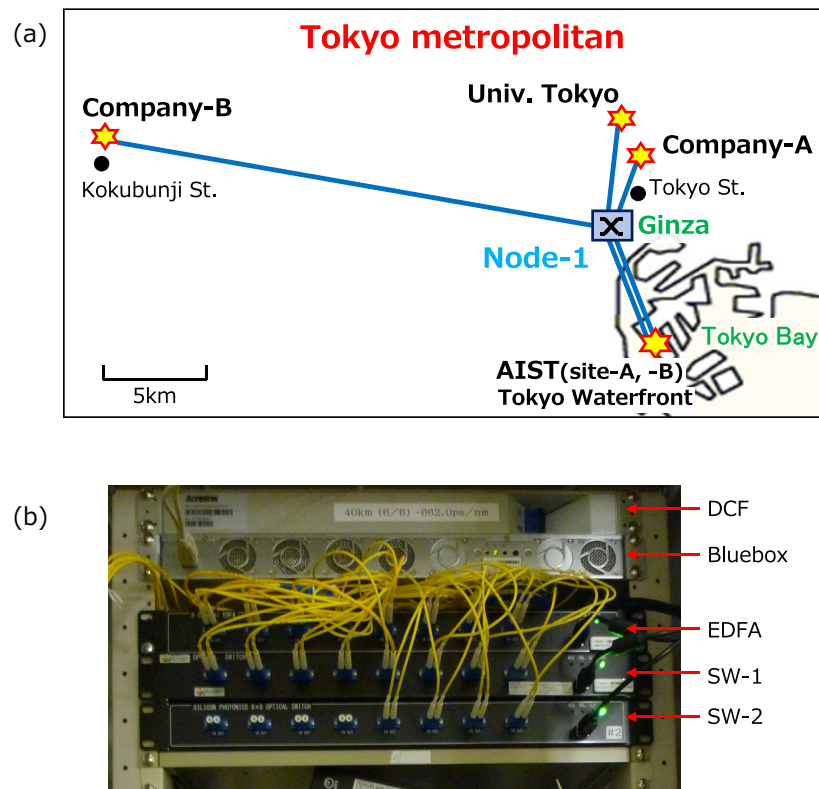


Fig. 1. DOPN testbed deployed in Tokyo metropolitan area. (a) Configuration of the network. Blue lines represent a link by a pair of fibres. (b) Photograph of instruments that compose Node-1.

So far, we have manufactured two Si-nanowire 8×8 switches, which have an insertion loss of approximately 12 dB. One is used in Node-1 and the other is used in Node-2, which will be described below. Fig. 1b shows the photograph of the instruments that compose Node-1: two 8×8 optical switches (SW-1, -2), an 8-ch EDFA, a dispersion compensation fibre (DCF: -660 ps/nm) and a node controller (code name: Bluebox). Here, SW-1 is a commercial MEMS switch and SW-2 is the

Si-nanowire switch. The 8-ch EDFA is used to compensate for the loss of the fiber link and the Si-nanowire optical switch. Bluebox plays a role to control optical devices obtained from different manufacturers using unified commands sent from a network manager system [11].

When we conducted system evaluation of the testbed, two spans (“site-B ↔ Node-1” and “Tokyo Univ. ↔ Node-1”) were unavailable. Thus, we temporally established a second optical node (Node-2) in site-A and a new link between the two sites of AIST (“site-A ↔ site-B”). Node-2 consisted of a Si-nanowire 8×8 switch (SW-3), 8-ch and 1-ch EDFAs, a DCF (-660 ps/nm) and three bandpass filters. The characteristics of each fiber link are shown in Table I.

Table I. Characteristics of fibre links used in the experiment.

Span	Fibre length	Loss
Node-1 ↔ Node-2	SMF: 14.8 km	9.5 dB
Node-1 ↔ Company-A	SMF: 13.3 km	7.8 dB
Node-1 ↔ Company-B	SMF: 14.1 km & DSF: 26.7 km	12.7 dB
Node-2 ↔ Site-B	SMF: 0.1 km	1 dB

3 Experiment and results

We studied long-term system performance of the testbed using two field testers (FT-1, -2) placed in site-A. The configuration of optical path used in the experiment is shown in Fig. 2. To emulate a large scale optical path network, we made up optical paths at Node-1 and Node-2 in such a way that transmitted signals went through optical switches as many times as possible. In Node-2, signals went through all the ports of SW-3. Whereas, signals went through SW-1 twice and SW-2 once at every passage through Node-1. As a result, transmitted signals went through optical switches 14 times in total (10 times through the Si-nanowire switch). We note that only four input/output ports were used in SW-2 because other ports were reserved for future users.

FT-1 and FT-2 generated 10-Gb/s OOK signals (PRBS: $2^{15}-1$) at 1538.2 nm (ch.1) and 1539.0 nm (ch.2), respectively. The two signals were multiplexed by a 3-dB optical coupler. A preliminary experiment showed that error free transmission is achieved if signal with nominal output power is transmitted. Therefore, the signal from TF-2 was attenuated before multiplexing so that temporal variation of the error rate could be monitored. The signal power was -4.4 dBm and -11.0 dBm for ch.1 and ch.2, respectively. The WDM signals were guided to Node-2, where the signals were transmitted to Node-1 after passing SW-3 three times. At Node-1, two switches (SW-1 and SW-2) directed the signals to company-A or company-B, from where the signals were returned to Node-1. At Node-1, the signals were transmitted to Node-2 in site-A and then transmitted to site-B after passing SW-3 four times. At site-B, the signals were sent back to Node-2 and then guided to measurement section by SW-3. In the measurement section, the two channels were demultiplexed by a wavelength selective switch (WSS) and fed to the field tester for bit-error-rate (BER) measurement. The received signal power was -3.7 dBm and -9.6 dBm for

ch.1 and ch.2, respectively. The optical spectra of the received signals are shown in Fig. 3.

In the experiment, room temperature was controlled in the location of Node-1. However, to conduct the evaluation under non-ideal condition, temperature control was turned off in site-A, where Node-2 and FTs were located. Although environmental changes in site-A (temperature, pressure, humidity, etc.) were not monitored, we recognized that room temperature changed more than 10 degree and received signal power changed by approximately 0.5 dB under this condition.

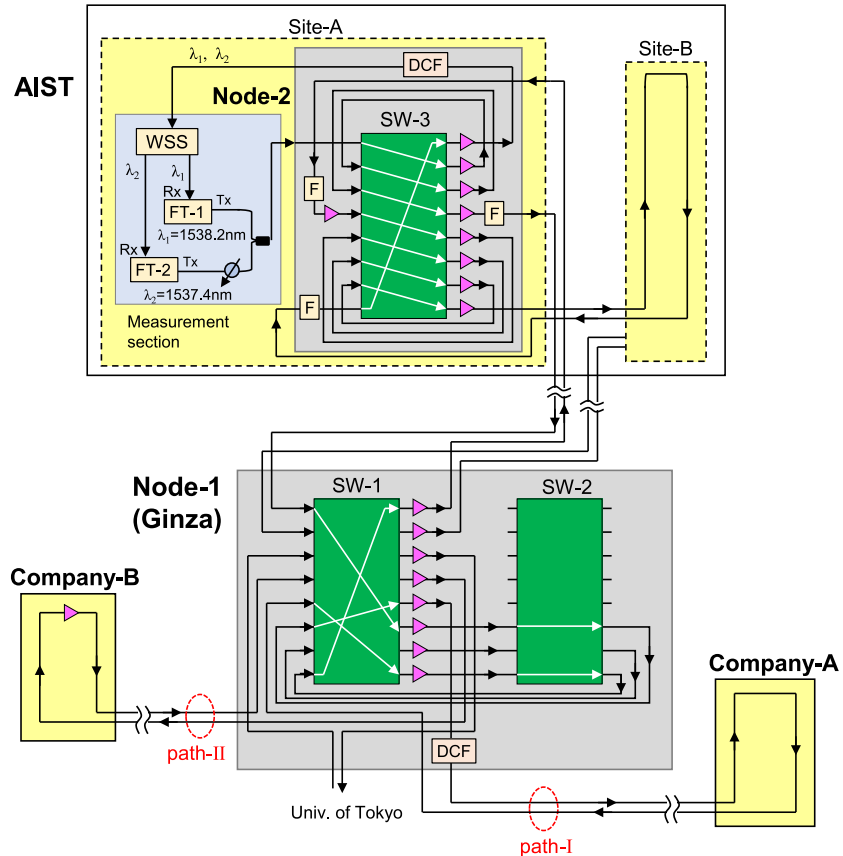


Fig. 2. Experimental setup. White arrows in SW-1, -2, -3 show the path settings when path-I is selected. FT: Field tester, WSS: Wavelength selective switch, DCF: Dispersion compensating fibre, F: Optical bandpass filter.

We studied transmission characteristics for two optical paths (path-I and path-II) by recording error count every 2 hours. In path-I, the signals transmitted from Node-2 to Node-1 were transmitted to company-A and returned to Node-1. In path-II, the signals transmitted from Node-2 to Node-1 were transmitted to company-B, where the signals were returned to Node-1 after amplification by an EDFA. In both optical paths, signals went through Si-nanowire switches 10 times in total (8 times in SW-3 and 2 times in SW-2). In Fig. 2, path settings of SW-1, -2, -3 in the case of path-I are indicated as an example.

Fig. 4 shows the temporal variation of BER measured for two channels over a week. Here, BER was calculated based on the error count made in 2-hour measurement time, which limited the lowest measurable BER to 1.4×10^{-14} . The measure-

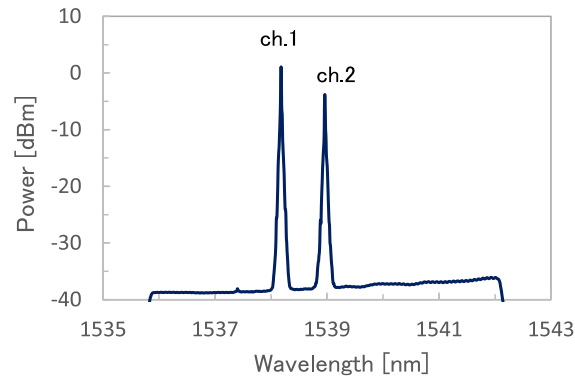


Fig. 3. Optical spectra of the received signals.

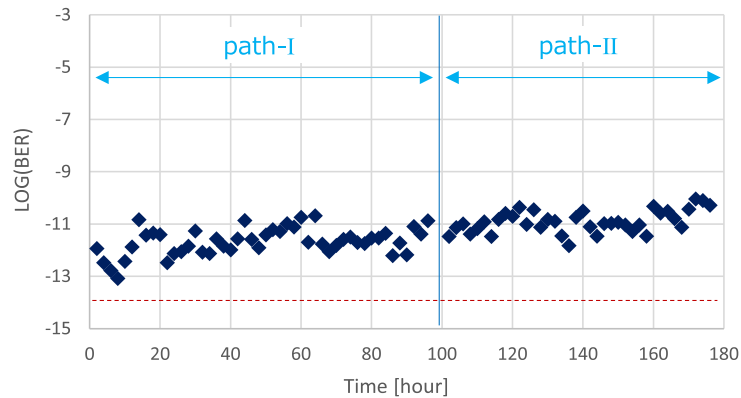


Fig. 4. Temporal variation of BER measured for ch.1 (—) and ch.2 (◆).

ment was started with path-I and, four days later, path was switched to path-II. During the BER measurement, optical path was switched once by SW-1 while other switches (SW-2 and SW-3) were operated in the same switch state. Error counting was suspended during the period of path switching because received signals were lost. For ch.1, transmitted power (P_T) and received power (P_R) were -4.4 dBm and -3.7 dBm, respectively. At this condition, no error was counted throughout the measurement period and lowest limit (1.4×10^{-14}) is plotted as the measured value of BER. For ch.2, signal transmission was performed with very small power: $P_T = -11.0$ dBm and $P_R = -9.6$ dBm. In spite of the very bad condition, measured BER was always below 10^{-9} with variation between 10^{-13} and 10^{-10} . This suggests that the two Si-nanowire switches were operating nearly in the optimum condition. In this measurement, BER was very sensitive to the received signal power because SNR was very low due to severely reduced transmitted signal power and multiple amplification by the EDFAs (13 times in path-I and 14 times in path-II). In path-II, measured BER is slightly worse than in path-I, because signals experienced one more amplification by an EDFA. There is a degrading tendency in the long-term BER performance of ch.2. The reason for this is not clear, but it can be accounted for if the received signal power decreased by ~ 0.5 dB during the measurement.

4 Discussions

The stable transmission characteristics observed in the DOPN testbed shows that

two Si-nanowire 8×8 switches were operating properly without any adjustment for a long time of period. The evaluation was performed in a severe condition, where WDM signals transmitted silicon photonics switches 10 times in cascade. Specifically, SW-3 was operated with all ports loaded condition. These results show that optical switches based on Si-nanowire waveguide allow long-term reliable operation without any active control of the switch elements. This is a big advantage in designing large scale optical switches.

We noted that the two silicon photonics switches have been used with no adjustment or update of the look-up table for more than a year since they were fabricated. During this time, one of the switches (SW-2) was shipped to/from USA for the exhibition of an international conference (OFC2017, Los Angeles, 2017). This suggests that the switches are robust enough against transportation and environmental change. In addition, the stable performance presented here was achieved by optical switches that employed off-chip polarization-diversity using external PBSs. It is expected that robustness and reliability would be enhanced in the optical switches employing on-chip polarization-diversity scheme [12].

5 Conclusion

We operated two Si-nanowire 8×8 switches in the optical nodes of Tokyo metropolitan DOPN testbed, where two optical paths was configured so that signals went through Si-nanowire switches 10 times in total. Error free transmission of 10-Gb/s WDM signal was achieved for a week, during which optical path was switched from path-I to path-II. The results suggest that optical switches based on Si-nanowire waveguide is available for practical application without employing active control of switch elements.

Acknowledgments

Part of this work was supported by Project for Developing Innovation Systems of the Ministry of Education, Culture, Sports, Science and Technology (MEXT), Japan.